Phosphorylation of Human Tau Protein by Microtubule Affinity-Regulating Kinase 2

Martin Schwalbe,[†] Jacek Biernat,[‡] Stefan Bibow,[||] Valéry Ozenne,[⊥] Malene R. Jensen,[⊥] Harindranath Kadavath,[||] Martin Blackledge,[⊥] Eckhard Mandelkow,[‡,§] and Markus Zweckstetter*[,†,||,@]

[†]German Center for Neurodegenerative Diseases (DZNE), 37077 Göttingen, Germany
[‡]German Center for Neurodegenerative Diseases (DZNE), 53175 Bonn, Germany
[§]CAESAR Research Center, Ludwig-Erhard-Allee 2, 53175 Bonn, Germany
[||]Department for NMR-based Structural Biology, Max Planck Institute for Biophysical Chemistry, 37077 Göttingen, Germany
[⊥]Protein Dynamics and Flexibility, Institut de Biologie Structurale Jean-Pierre Ebel, CEA, CNRS, 38027 Grenoble, France
[@]Center for Nanoscale Microscopy and Molecular Physiology of the Brain, University Medical Center, 37073 Göttingen, Germany

S Supporting Information

ABSTRACT: Tau protein plays an important role in neuronal physiology and Alzheimer's neurodegeneration. Its abilities to aggregate abnormally, to bind to microtubules (MTs), and to promote MT assembly are all influenced by phosphorylation. Phosphorylation of serine residues in the KXGS motifs of Tau's repeat domain, crucial for MT interactions and aggregation, is facilitated most efficiently by microtubule-associated protein/microtubule affinity-regulating kinases (MARKs). Here we applied high-resolution nuclear magnetic resonance analysis to study the kinetics of phosphorylation of Tau by MARK2 and its impact on the structure and microtubule binding of Tau. We demonstrate that MARK2 binds to the N-terminal tail of Tau and selectively phosphorylates three major and five minor serine residues in the repeat domain and C-terminal tail. Structural changes induced by phosphorylation of Tau by MARK2 are highly localized in the proximity of the phosphorylation site and do not affect the global conformation, in contrast to phosphorylation in the proline-rich region. Furthermore, single-residue analysis of binding of Tau to MTs provides support for a model in which Tau's hot spots of MT interaction bind independently of each other and are differentially affected by phosphorylation.
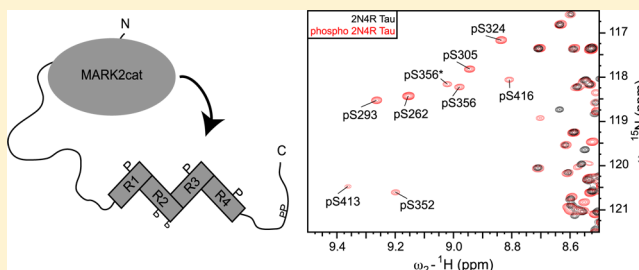
Neurodegenerative tauopathies are a group of diseases marked by the accumulation of hyperphosphorylated Tau, intracellular Tau deposits, abnormal Tau splicing, and Tau gene mutations.[1] Among others, this group includes disorders such as Alzheimer's disease (AD), frontotemporal dementia with parkinsonism linked to chromosome 17, Pick disease, and progressive supranuclear palsy (PSP).[2] The physiological role of Tau is to regulate the assembly and stability of microtubules (MTs) in the axons of neurons of the central nervous system (CNS).[3] Tau is therefore important for axonal development and intracellular transport.[4] In addition, other cellular roles of Tau have been described.[5]

In the human CNS, Tau is expressed in six isoforms because of alternative splicing of exons 2, 3, and 10. The isoforms differ by the inclusion of the second tubulin-binding repeat, R2, giving rise to three or four repeat-containing Tau isoforms (3R or 4R Tau) and have either zero (0N Tau), one (1N Tau), or two (2N Tau) N-terminal inserts (N1 and N2). The lack of stable secondary structure[6] and its resistance to heat and acid denaturation[7] classify Tau as a natively unfolded or intrinsically disordered protein (IDP).[8] Using nuclear magnetic resonance (NMR) spectroscopy, we have previously identified transient

elements of secondary structure in Tau.[9] In addition, transient contacts between different Tau domains were revealed by NMR, Förster resonance energy transfer, and other methods.[9,10]

The ability of Tau to bind to MTs and promote their assembly is regulated by post-translational modifications, in particular by phosphorylation.[11] Depending on the position and number of phosphorylated residues, different effects on MT polymerization and MT binding are observed. Whereas phosphorylation of either Ser-214,[12] Thr-231,[13,14] or Ser-262[15] decreases the affinity for MTs and inhibits Tau's MT assembly ability, phosphorylation of either Ser-202/Thr-205, Ser-235, or Ser-396/Ser-404 has little effect on MT binding but abolishes the ability of MTs to self-assemble.[16,17] Of particular importance is phosphorylation of Ser-262, which is localized in the first repeat domain of Tau within a conserved KXGS motif. Ser-262 phosphorylation is thought to be at the top of the phosphorylation cascade leading to Tau hyperphosphorylation

and preceding phosphorylation of Ser-202, Thr-205, Ser-396, and Ser-404.[18] Phosphorylation of Tau with brain extract facilitates extensive phosphorylation at Ser-262 and the other KXGS motifs in the repeat domain, as well as many proline-directed phosphorylation sites in the flanking regions.[15,19] Mutation of Ser-262 to alanine largely rescues the MT assembly properties of Tau that are lost when wild-type Tau is phosphorylated by brain extracts. Moreover, mutation of Ser-262 and Ser-356 residues to alanine in cell and animal models rescues the toxic effects of this type of phosphorylation for neuronal cells but on the other hand inhibits the outgrowth of neuronal processes highlighting the importance of these phosphorylation sites for neuronal differentiation.[20−22]

Several kinases have been described to phosphorylate Tau *in vitro* at the KXGS motifs; however, most kinases phosphorylate several sites to varying extents.[23] This is particularly true for Tau, because of its unfolded structure and its large number of potential phosphorylation sites (up to 85 phosphorylatable residues). Preferential phosphorylation of the KXGS motifs is facilitated by the microtubule-associated protein (MAP)/microtubule affinity-regulating kinases (MARKs) and other members of the family of adenosine monophosphate-activated protein kinases.[24] MARK kinases (MARK1−4) were originally discovered as regulators of MT stability and are important for the maintenance of neuronal polarity and other processes in neuronal differentiation. In particular, MARK2 is essential for axon formation and neuronal migration.[25] Furthermore, selective inhibition of MARK family members abrogates toxic effects induced by Aβ.[22]

A major problem in investigating the type and function of phosphorylation sites in Tau has been their incomplete detection and quantitation. This is caused by the limited availability of phospho-site-specific antibodies, variable affinities (usually unknown), and a lack of defined controls (i.e., antibodies against specific nonphosphorylated sites). NMR analysis bypasses this problem because it allows the simultaneous detection of multiple sites in their phosphorylated and nonphosphorylated forms, as well as the time course of phosphorylation.[26] Here we analyzed the kinetics and relative extent of phosphorylation of Tau (2N4R) by MARK2, as well as the impact of Tau phosphorylation on its structure and MT binding. We demonstrate that MARK2 directly binds to the N-terminal tail of 2N4R Tau and selectively phosphorylates up to eight serine residues (three primary, two secondary, and three minor sites). Structural changes induced by phosphorylation of Tau by MARK2 are highly localized in the proximity of the phosphorylation sites and do not affect the global paperclip conformation.[27] Furthermore, single-residue analysis of binding of Tau to MTs provides support for a model in which Tau's hot spots of MT interaction bind independent of each other and are differentially affected by phosphorylation.

■ EXPERIMENTAL PROCEDURES

Protein Preparation and Peptide Synthesis. The preparation of full-length 2N4R Tau and Tau peptide Tau(254−284) comprising residues 254−284 is described in the Supporting Information.

Phosphorylation of Tau. With the aim of achieving a high degree of phosphorylation, 2N4R Tau was incubated at 30 °C with MARK2cat-T208E at a Tau:MARK2 ratio of 10:1 for 8 h. The buffer contained 25 mM 2-[4-(2-hydroxyethyl)piperazin-1-yl]ethanesulfonic acid (pH 8.0), 100 mM NaCl, 5 mM MgCl$_2$, 2 mM ethylene glycol tetraacetic acid (EGTA), 1 mM

dithiothreitol (DTT), 1 mM benzamidine, 0.5 mM phenyl-methanesulfonyl fluoride (PMSF), and 1 mM ATP. After phosphorylation, Tau samples were buffer exchanged with 50 mM NaH$_2$PO$_4$/Na$_2$HPO$_4$ (pH 6.8) and 10% (v/v) D$_2$O. For real-time phosphorylation of 2N4R Tau by MARK2cat, the temperature was decreased to 25 °C and the buffer changed to 25 mM NaH$_2$PO$_4$/Na$_2$HPO$_4$ (pH 6.8), 100 mM NaCl, 5 mM MgCl$_2$, 2 mM EGTA, 1 mM DTT, 1 mM benzamidine, 0.5 mM PMSF, 1 mM ATP, and 5% (v/v) D$_2$O. In addition, the Tau:kinase ratio was increased to 40:1.

NMR Spectroscopy. NMR spectra were acquired at field strengths of 900, 800, 700, and 600 MHz on spectrometers equipped with Bruker 5 mm cryogenic or room-temperature, triple-resonance probeheads or a Bruker 1.7 mm cryogenic, triple-resonance probe. Unless stated otherwise, spectra were acquired at 5 °C. A description of the assignment of 2N4R Tau and Tau(254−284), determination of paramagnetic relaxation enhancement (PRE) profiles, and measurement of residual dipolar couplings (RDCs) is given in the Supporting Information. The *flexible-meccano*/ASTEROIDS approach for the ensemble description of the Tau(254−284) peptide is also described there.

Real-Time Phosphorylation of 2N4R Tau. A sample containing 100 μM ^{15}N-labeled 2N4R Tau was prepared as described above with a Tau:MARK2 ratio of 40:1 in buffer (pH 6.8). After the addition of kinase, the sample was transferred to a 5 mm Shigemi tube and phosphorylation was assessed by a series of ^{1}H−^{15}N heteronuclear single-quantum coherence (HSQC) spectra over a time period of approximately 15 h. Each HSQC experiment was conducted at 800 MHz and 25 °C with a duration of 30 min. Parameters were eight transients, sweep widths of 8.0 (^{1}H) × 2.0 (^{15}N) kHz, and 1024 (^{1}H) × 200 (^{15}N) total points. Carrier frequencies were set to the water resonance for ^{1}H and to 118 ppm for ^{15}N. To derive site-specific rate constants for the phosphorylation reaction, peak intensities were fit to a monoexponential function using IgorPro6.0 (Wavemetrics). Rate constants listed in Table 1 are the average of constants determined for nonoverlapped peaks near the phosphorylation site that show an intensity modulation. The standard deviation is shown as the error in Table 1. The degree of phosphorylation was calculated from the peak intensities of the phosphorylated residue divided by the

Table 1. Phosphorylation Kinetics of 2N4R Tau by MARK2[a]

| residue | MARK2cat-T208E, 30 °C, pH 8.0 | MARK2cat, 25 °C, pH 6.8 | |
	degree of phosphorylation (%)	degree of phosphorylation (%)	rate constant (h^{-1})
Ser-262	100 ± 1	100 ± 1	0.323 ± 0.025
Ser-293	84 ± 5	32 ± 3	0.037 ± 0.002
Ser-305	66 ± 2	20 ± 6	*b*
Ser-324	100 ± 1	100 ± 2	0.189 ± 0.019
Ser-352	46 ± 2	15 ± 5	*b*
Ser-356	100 ± 2	100 ± 2	0.458 ± 0.056
Ser-413	45 ± 8	14 ± 4	*b*
Ser-416	58 ± 8	38 ± 6	0.038 ± 0.006

[a]Degrees of phosphorylation and rate constants (only MARK2cat) determined from phosphorylation of 2N4R Tau by MARK2cat-T208E or MARK2cat. [b]Data for these residues could not be fit reliably because of the low peak intensities under the specific conditions. This sets an upper limit of the rate constants of approximately 0.03 h^{-1}.
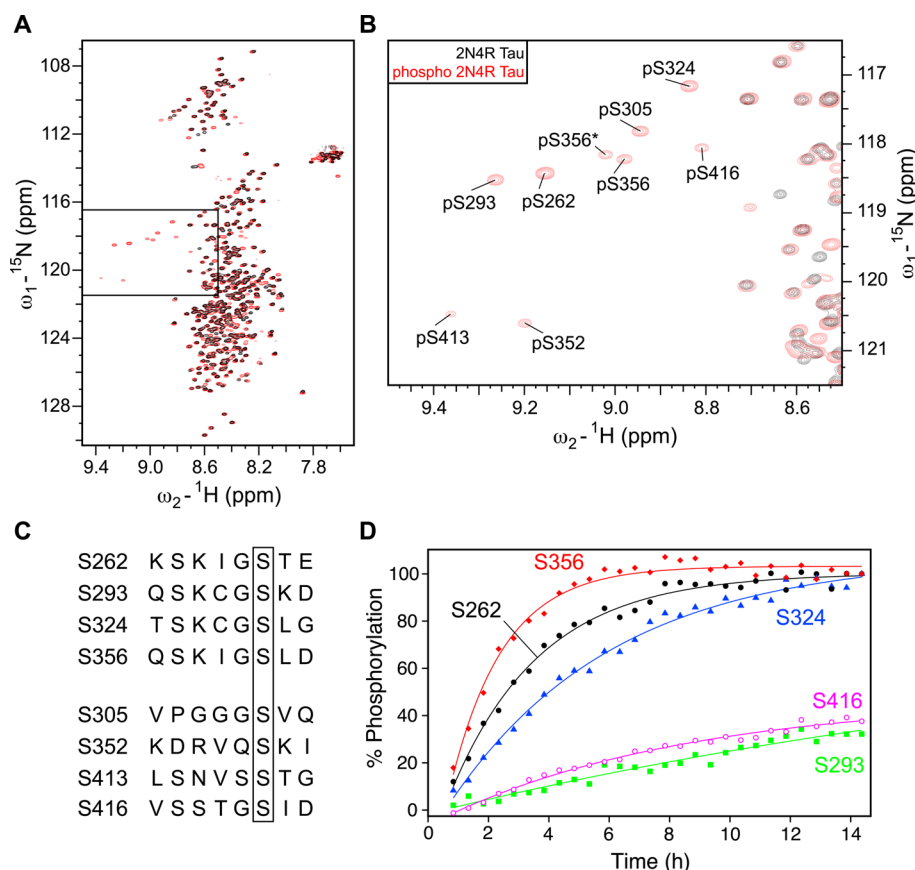
Figure 1. Phosphorylation of Tau by MARK2. (A) Comparison of the ^{1}H$-^{15}$N HSQC spectra of 2N4R Tau in its MARK2cat-T208E-phosphorylated (red contours) and nonphosphorylated state (black contours), both at 5 °C. 2N4R Tau was incubated with MARK2cat-T208E for 8 h. The spectral region with the eight phosphorylated serine residues is highlighted by a black rectangle, and a magnified view of this region is shown in panel B. Phosphorylation of Ser-352 causes a splitting of the resonance of phosphorylated Ser-356. Phosphorylated Ser-356 associated with phosphorylated Ser-352 is marked with an asterisk (pSer-356*). (C) Amino acid sequences of the regions each containing one phosphorylation site (marked by a rectangle). (D) Real-time kinetics of phosphorylation of 2N4R Tau by wild-type MARK2cat: Ser-356 (in R4, red diamonds), Ser-262 (in R1, black circles), Ser-324 (in R3, blue triangles), Ser-293 (in R2, green squares), and Ser-416 (in the C-terminus, magenta circles). Solid lines show fits obtained from the calculation of rate constants. Errors are <6% based on the signal-to-noise ratio. The phosphorylation kinetics of residues Ser-305, Ser-352, and Ser-413 could not be analyzed under the specific conditions (25 °C and pH 6.8) because of low NMR peak intensities (Table 1).

sum of the intensities of the phosphorylated and non-phosphorylated state.

Titration of 2N4R Tau with MARK2. To identify possible MARK2 interaction sites on Tau, ^{15}N-labeled 2N4R Tau was titrated with increasing amounts of MARK2cat. Using a Tau concentration of 15 μM, MARK2cat was added at concentrations of 37.5, 75, 150, and 225 μM (2.5-, 5-, 10-, and 15-fold molar excesses, respectively, of MARK2cat over 2N4R Tau). The buffer contained 25 mM NaH$_2$PO$_4$/Na$_2$HPO$_4$ (pH 6.8), 100 mM NaCl, 5 mM MgCl$_2$, 2 mM EGTA, 1 mM DTT, 1 mM benzamidine, 0.5 mM PMSF, 5% (v/v) glycerol, and 5% (v/v) D$_2$O. For each titration point, ^{1}H$-^{15}$N HSQC spectra were recorded at a spectrometer frequency of 800 MHz with the following settings: 64 transients, sweep widths of 8.0 (^{1}H) × 2.0 (^{15}N) kHz, and 1024 (^{1}H) × 512 (^{15}N) total points. Intensity changes were analyzed relative to a 2N4R Tau sample under identical conditions but without MARK2. Peak intensities were averaged over a three-residue window.

Microtubule Binding Assay. Paclitaxel-stabilized MTs were assembled as described previously.[9] Nonphosphorylated, MARK2cat-phosphorylated, and pseudophosphorylated[27] 2N4R Tau were incubated with MTs at a ratio of 2:1 for 30 min at 37 °C. Afterward, ^{1}H$-^{15}$N HSQC spectra were acquired

at field strengths of 800 and 900 MHz with 64 transients, sweep widths of 8.0 (^{1}H) × 2.0 (^{15}N) kHz, and 1024 (^{1}H) × 600 (^{15}N) total points. Peak intensities in the presence of MTs were normalized to the intensity in the absence of MTs and averaged over a three-residue window. Note that for all MT interaction studies, tubulin from the same stock and identical MT assembly conditions were used.

■ **RESULTS**

Phosphorylation of Tau by MARK2. To phosphorylate 2N4R Tau, we used a kinase construct that comprises only the catalytic domain of MARK2 (MARK2cat) but displays comparable *in vitro* substrate specificity.[28] Full-length MARK2 could not be expressed in *Escherichia coli* cells in quantities sufficient for phosphorylation of NMR samples. In addition to the wild-type catalytic domain, we also used the hyperactive MARK2cat-T208E variant.[29] At 30 °C and pH 8.0, MARK2cat-T208E selectively phosphorylated eight serine residues in the C-terminal half of 2N4R Tau (Figure 1A,B). Consistent with a previous study,[30] the eight sites included the four KXGS motifs in the repeat domains. While residues Ser-262, Ser-324, and Ser-356 were completely phosphorylated, Ser-293 in the second
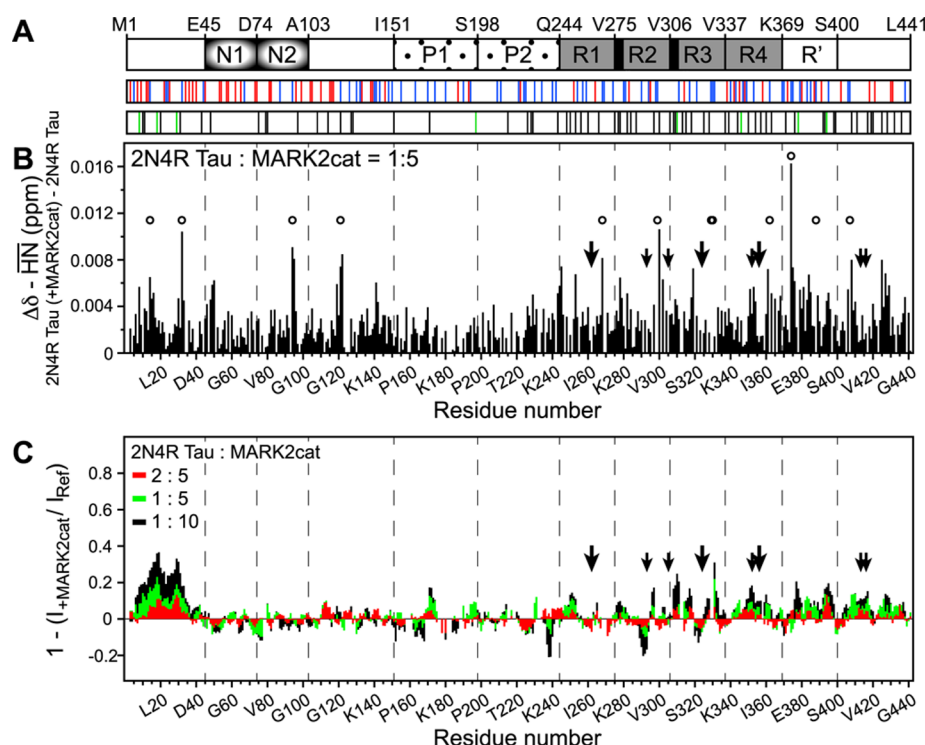
Figure 2. Binding of MARK2cat to Tau. (A) Domain structure of 2N4R Tau. Shown are the two N-terminal inserts (N1 and N2, black boxes with white centers), the two proline-rich domains (P1 and P2, dotted boxes), and the four pseudorepeats (R1−R4, gray boxes). The two hexapeptides motifs with high β-strand propensity at the N-terminal beginning of R2 and R3 are displayed as black rectangles. Shown below the domain structure is the distribution of positively (blue) and negatively (red) charged residues, as well as the location of hydrophobic [I, M, L, and V (black bars)] and aromatic [F and Y (green bars)] residues. (B and C) Changes in NMR signal position (B) and intensity (C) in 2N4R Tau upon addition of increasing amounts of MARK2cat. [Note that spikes in panel B at a Tau:MARK2cat ratio of 1:5 stem from histidine residues (marked by circles), which probably are due to slight differences in pH.] NMR signal intensities in the presence of MARK2cat were normalized to the reference of 2N4R Tau without MARK2cat and subtracted from one. Tau:MARK2cat ratios were 2:5 (red bars), 1:5 (green bars), and 1:10 (black bars). Vertical dashed lines mark the domain boundaries in Tau. Black arrows mark the eight MARK2cat-phosphorylated serine residues (larger arrows for primary sites Ser-356, Ser-262, and Ser-324) (Table 1).

repeat was only 84% phosphorylated (Table 1). Furthermore, four non-KXGS phosphorylation sites were detected, two within the repeat domain (Ser-305 in R2 and Ser-352 in R4) and two more at the C-terminus (Ser-413 and Ser-416) (Figure 1B,C). Of these, Ser-305 was 66% phosphorylated and Ser-352, Ser-413, and Ser-416 were ∼45−58% phosphorylated (Table 1). Using wild-type MARK2cat at 25 °C and pH 6.8, the same phosphorylation sites were observed. The three primary sites, Ser-262, Ser-324, and Ser-356, were still completely phosphorylated. However, Ser-293 and Ser-416 were only 30−40% phosphorylated, and the three minor sites, Ser-305, Ser-352, and Ser-413, were only 20% phosphorylated (Table 1). We attribute the observed difference to the lower catalytic activity of MARK2cat and less favorable reaction conditions [the pH and temperature were slightly reduced for the real-time phosphorylation to allow for sensitive NMR detection (for details, see Experimental Procedures)].

Analysis of Tau phosphorylation by NMR spectroscopy is uniquely suited to investigation of the kinetics of phosphorylation. Indeed, a kinetic analysis revealed differences in the rate constants of phosphorylation with efficiency decreasing in the following order: Ser-356 > Ser-262 > Ser-324 > Ser-416 to Ser-293 (Table 1 and Figure 1D). The phosphorylation reaction was most efficient for the two KIGS motifs (0.458 h^{-1} for Ser-356 and 0.323 h^{-1} for Ser-262), whereas Ser-293 and Ser-324 within the KCGS motifs had significantly smaller rate constants (0.037 and 0.189 h^{-1}, respectively). Notably, Ser-262 and Ser-

356 have different phosphorylation kinetics, despite having the same recognition motif (KIGS).

MARK2cat Binds to the N-Terminal Tail of Tau. NMR signal intensities and chemical shifts are sensitive probes for biomolecular interactions.[31] To gain more insight into the interaction of MARK2 and 2N4R Tau, 2N4R Tau was titrated with increasing amounts of MARK2cat in the absence of ATP, i.e., when no phosphorylation can occur. Addition of MARK2cat induced small chemical shift changes and resonance broadening (Figure 2A−C), suggesting that the binding reaction is intermediate on the NMR time scale. Some of these changes mapped to the C-terminal half of 2N4R Tau where the phosphorylation sites are located. Comparison with the distribution of hydrophobic and aromatic residues (Figure 2A) suggests that the binding sites are related to the presence of these amino acid types. Most pronounced, however, was the signal broadening of residues 8−33 at the N-terminus of Tau (Figure 2C), indicating that residues 8−33 have the highest affinity for MARK2cat.

Structural Impact of the Phosphorylation by MARK2 on 2N4R Tau. Comparison of NMR chemical shift differences between phosphorylated and nonphosphorylated 2N4R Tau indicates that Tau remained disordered after phosphorylation by MARK2 (Figures 1A and 3A). Elements of rigid secondary structure were not induced. However, 8−10 residues up- and downstream from the phosphorylation site were affected (Figure 3A−C). Toward the N-terminal end from the
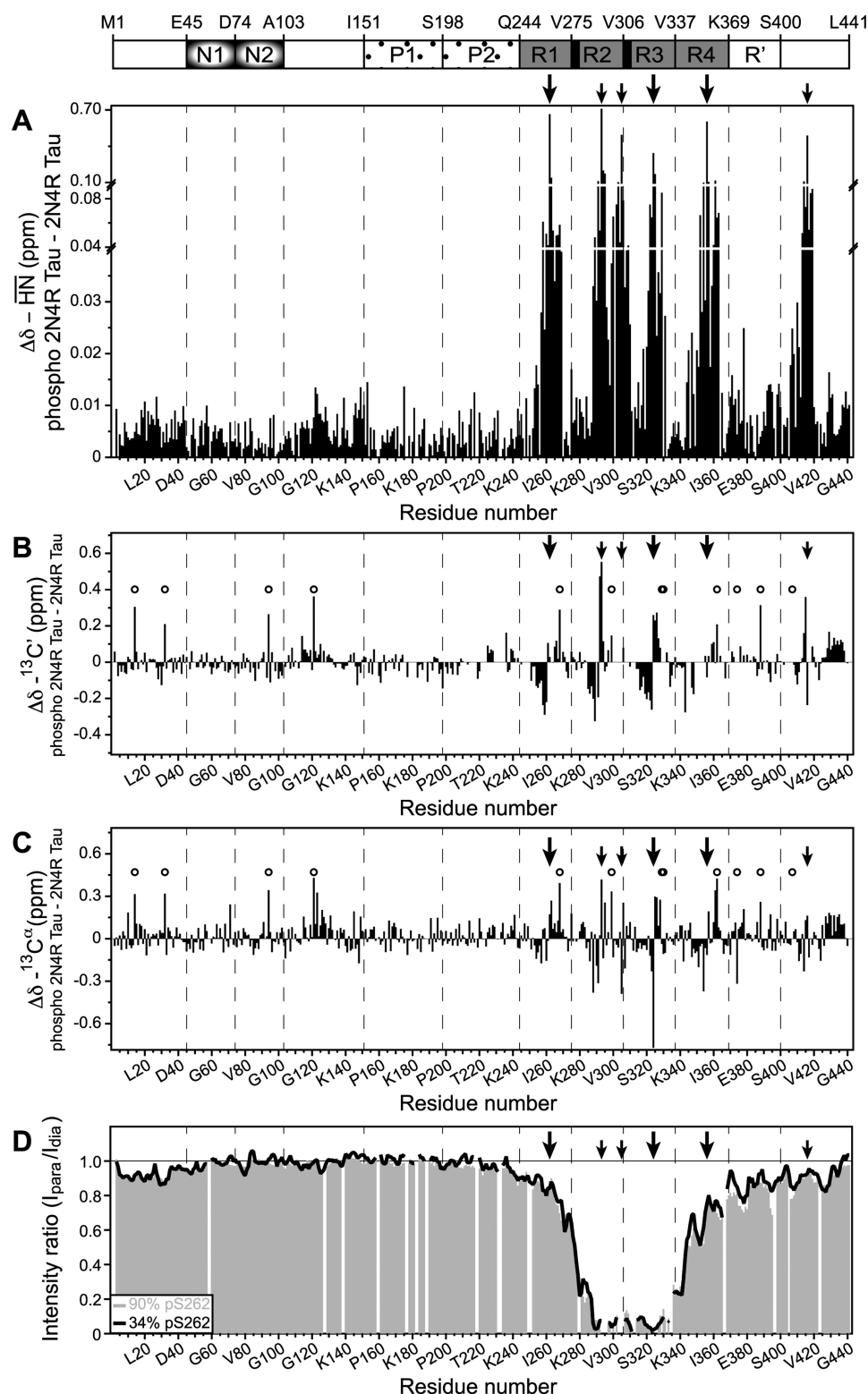
Figure 3. Phosphorylation-dependent structural changes in 441-residue Tau. Chemical shift differences between 2N4R Tau phosphorylated by MARK2cat-T208E and nonphosphorylated Tau are shown for the normalized weighted average of $^1H^N$ and ^{15}N shifts (A), $^{13}C'$ shifts (B), and $^{13}C^\alpha$ shifts (C). Major chemical shift perturbations are observed next to the phosphorylation sites. The six strongest phosphorylation sites, Ser-262, Ser-293, Ser-305, Ser-324, Ser-356, and Ser-416 (Table 1), are highlighted by black arrows (larger arrows for primary sites Ser-356, Ser-262, and Ser-324). The domain structure of 2N4R Tau is shown at the top. Vertical dashed lines mark domain boundaries. Spikes in the N-terminal half of 2N4R Tau in panels B and C stem from histidine residues (marked by circles) and are due to slight differences in pH. (D) Comparison of PRE profiles of highly phosphorylated 2N4R Tau with Ser-262 ~90% phosphorylated (gray bars) with the profile of a modestly phosphorylated 2N4R Tau with Ser-262 ~34% phosphorylated (black line). The MTSL label was attached to native cysteines Cys-291 (in R2) and Cys-322 (in R3) in 2N4R Tau. Residues within ~25 Å of the spin-label experience a distance-dependent line broadening; however, no long-range conformational changes are observed upon phosphorylation by MARK2cat.
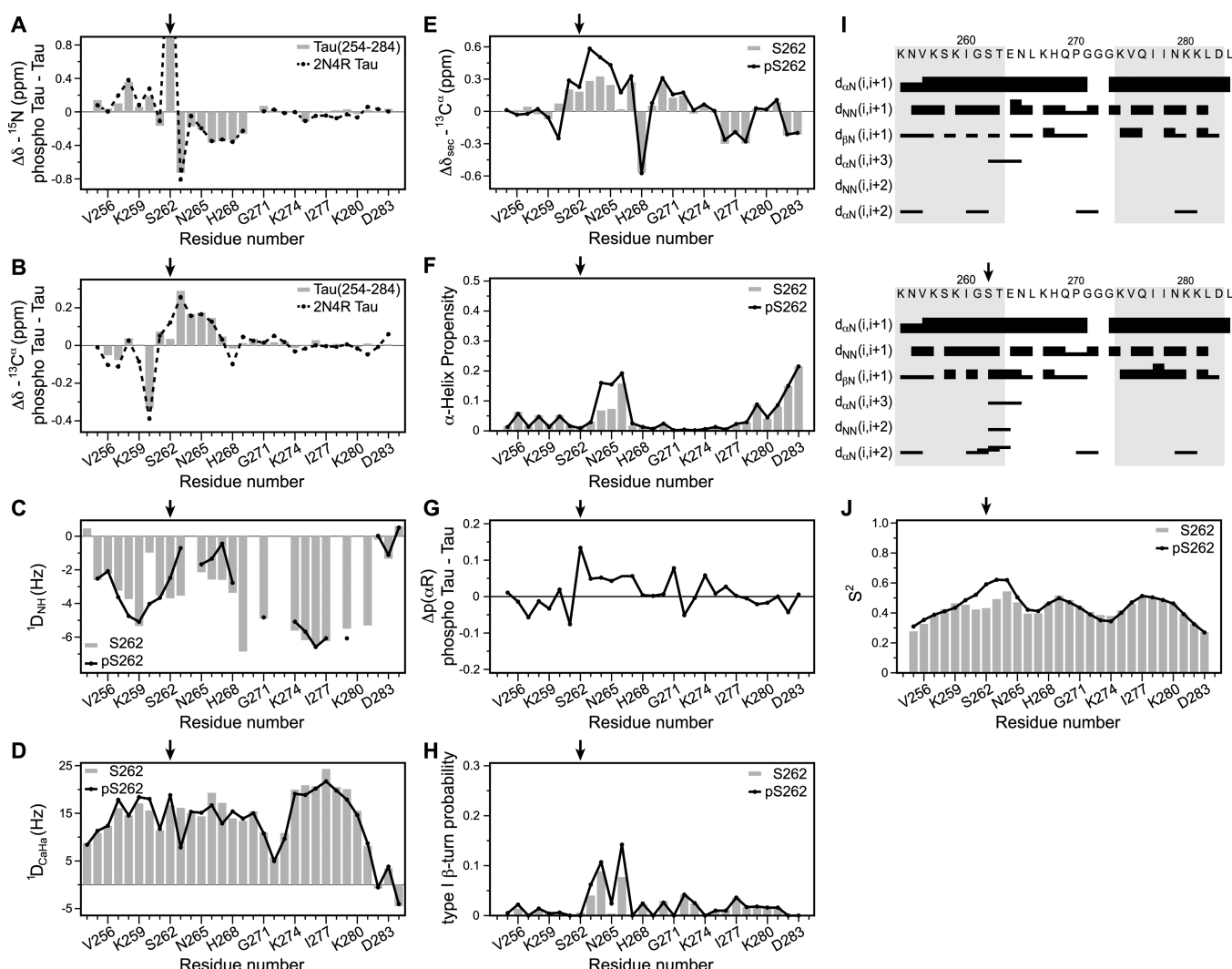
Figure 4. Structural consequences of Ser-262 phosphorylation. Chemical shift differences between phosphorylated and nonphosphorylated 2N4R Tau (dashed black line) and Tau(254−284) (gray bars) are shown for the backbone amide ^{15}N (A) and the $^{13}C^\alpha$ atom (B). (C) $^{1}D_{NH}$ and (D) $^{1}D_{CaHa}$ RDCs of Ser-262-phosphorylated (black line) and nonphosphorylated (gray bars) Tau(254−284). The same color coding is used for panels D−H and J. Errors for $^{1}D_{NH}$ RDCs are <1 Hz and those for $^{1}D_{CaHa}$ RDCs <1.3 Hz. (E) Secondary C^α chemical shifts ($\Delta\delta_{sec}$) of Tau(254−284) and Tau(254−284) phosphorylated at Ser-262. (F−H) Structural propensities of Ser-262-phosphorylated and nonphosphorylated Tau(254−284) calculated from chemical shifts using MICS.[34] (F) α-Helical propensity and (H) propensity to be the second residue within a type I β-turn. (G) Difference (phosphorylated minus nonphosphorylated) in the population of the α-helical region of the Ramachandran space [$\Delta p(\alpha R)$] as determined using the ASTEROIDS approach.[35] (I) Summary of sequential and medium-range NOEs in Tau(254−284) (top) and Tau(254−284)pS262 (bottom). (J) S^2 order parameters of Ser-262-phosphorylated and nonphosphorylated Tau(254−284) calculated from chemical shifts using MICS. Pronounced structural differences between Ser-262-phosphorylated and nonphosphorylated Tau(254−284) are present for residues 258−267. Black arrows mark the position of Ser-262 in all panels.

phosphorylated serine in the KXGS motifs, $^{13}C'$ and $^{13}C^\alpha$ chemical shifts were upfield shifted, while downstream residues showed a downfield shift (Figure 3B,C). In addition to the local changes and despite the absence of a nearby phosphorylation site, $^{13}C'$ and $^{13}C^\alpha$ atoms of residues 428−439 at the C-terminus of Tau, which transiently populate α-helical conformations,[9] were also affected (Figure 3B,C).

To probe the effect of MARK2 phosphorylation on the network of transient long-range interactions in Tau, we used paramagnetic relaxation enhancement (PRE). To this end, we attached nitroxide labels to the native cysteines at positions 291 and 322. We then compared PRE intensity profiles of a highly phosphorylated 2N4R Tau (~90 ± 1% phosphorylated Ser-262) and 2N4R Tau with a modest degree of phosphorylation (~34 ± 2% phosphorylated Ser-262). Comparison of the

moderately and highly phosphorylated state has the advantage that buffer conditions are identical, thereby preventing potential buffer-specific changes in the PRE profile. The PRE profiles of the two phosphorylated Tau species were virtually identical (Figure 3D). Thus, the small change in helical propensity for L428-Q439 did not lead to a detectable change in global structure.

To obtain further insight into phosphorylation-induced structural changes and to reduce the extent of NMR resonance overlap, we analyzed the structure of the Tau peptide comprising residues 254−284 [Tau(254−284)]. Phosphorylation at Ser-262 induced almost identical chemical shift changes in Tau(254−284) and 2N4R Tau (Figure 4A,B), supporting the relevance of the peptide study. We then measured $^{1}D_{NH}$ and $^{1}D_{CaHa}$ residual dipolar couplings (RDCs) that are highly
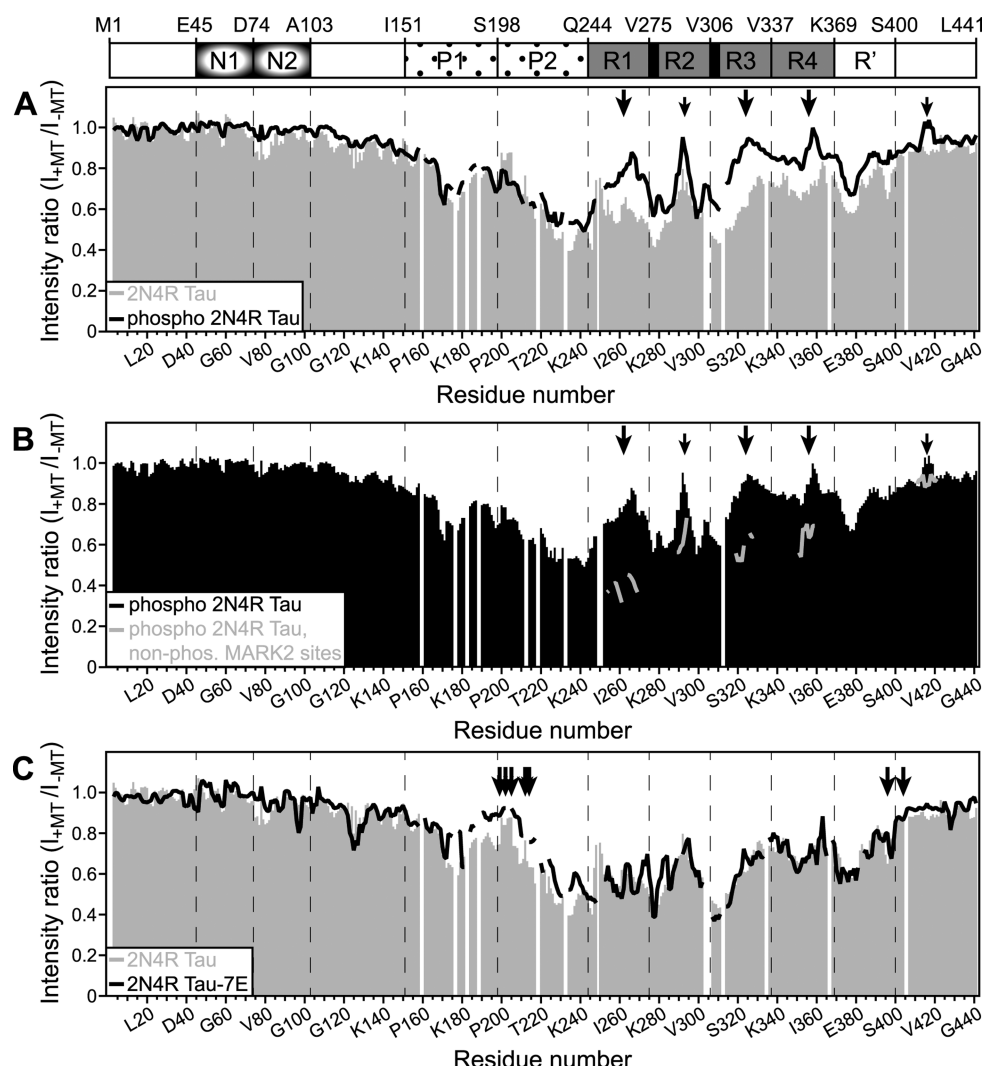
Figure 5. Phosphorylation-dependent modulation of the Tau—microtubule interaction. (A) Residue-specific intensity ratios in 2N4R Tau, which was phosphorylated by MARK2cat to ~72% at Ser-262 (black line), between the MT-bound and unbound state. Serines >25% phosphorylated by MARK2cat are denoted with arrows (larger arrows for primary sites Ser-356, Ser-262, and Ser-324). (B) Intensity ratios of nonphosphorylated residues from this partially MARK2cat-phosphorylated 2N4R Tau sample (gray line). For comparison, the resonance broadening of the phosphorylated form is shown (black bars). Increased signal intensities in the repeat region of MARK2cat-phosphorylated 2N4R Tau are the result of an impaired MT interaction. The domain structure is shown at the top. Vertical dashed lines mark domain boundaries. (C) Intensity ratios for the 2N4R Tau-7E variant (black line), which was pseudophosphorylated at the AT8, AT100, and PHF1 epitopes (denoted with arrows), between the MT-bound and unbound state. MT-induced resonance broadening of nonphosphorylated wild-type 2N4R Tau is shown for comparison (gray bars).

sensitive reporters of structure.[32] The largest phosphorylation-induced changes in RDCs were observed for residues Ser-258, Ile-260, Ser-262, Thr-263, Leu-266, and Lys-267 (Figure 4C,D). In line with the distinct chemical shift changes (Figure 4A,B,E), $^{1}D_{HN}$ RDCs of residues N-terminal to Ser-262 became more negative upon phosphorylation, while the magnitude of RDCs for C-terminal residues decreased (Figure 4C). Notably, in a charged alignment medium, we previously observed sign inversion of $^{1}D_{HN}$ RDCs of Asn-265, Leu-266, and Lys-267 upon pseudophosphorylation at Ser-262.[33] In the case of true phosphorylation and using the neutral alignment medium formed by polyethylene glycol, we did not find evidence of RDC sign inversion (Figure 4C). However, the decrease in the RDC magnitude is in line with a phosphorylation-induced shift to more helical or turnlike structures for residues 265−267.

Structural properties of Tau(254−284) were further studied by subjecting $^{1}H^{N}$, $^{1}H^{\alpha}$, ^{15}N, $^{13}C^{\alpha}$, and $^{13}C^{\beta}$ chemical shifts to MICS[34] and the chemical shifts together with RDCs to the

program *flexible-meccano*.[35] Both analyses indicated that residues 264−266 have an increased propensity for helixlike conformations upon phosphorylation at Ser-262 (Figure 4F,G), in line with the downfield shift of C^{α} atoms of these residues (Figure 4E). The chemical shift analysis suggested that residues 263−266 also transiently populate type I β-turn conformations prior to phosphorylation, which are enhanced upon phosphorylation (Figure 4H). The change of residues C-terminal to the phosphorylation site to turnlike and helical conformations was further supported by a medium-range NOE (nuclear Overhauser effect) contact between Ser-262 and Glu-264 (Figure 4I). In addition, the chemical shift analysis revealed that in the direct proximity of the site of phosphorylation the order parameter was increased (Figure 4J), indicating that phosphorylation rigidifies the backbone.

Site-Selective Modulation of MT Binding by Phosphorylation. Because of the importance of phosphorylation of Tau for MT binding, the upregulation of phosphorylation in

disease, and the potential contribution of impaired MT binding to neurotoxicity, the mechanism of binding of Tau to MTs is of great interest.[5] We previously showed that NMR spectroscopy can provide unique information about the interaction of Tau with MTs.[9,36] MT-binding sites in Tau can be identified from a decrease in the NMR signal intensity of residues involved in the interaction, whereas noninteracting residues show little intensity modulation. The NMR line broadening, in combination with changes in NMR signal position, is due to an exchange between free and MT-bound Tau that occurs on an intermediate NMR time scale.

To obtain insight into the consequences of phosphorylation on the MT interaction of Tau, we probed binding of phosphorylated Tau to preassembled MTs using NMR spectroscopy. First, the effect of phosphorylation was analyzed using MARK2 kinase activity operating mainly at KXGS motifs within the repeats. Phosphorylation of Tau by MARK2cat weakened the signal broadening in the repeat domain compared to that of the nonphosphorylated protein (Figure 5A). In particular for residues in the proximity of Ser-262, Ser-324, and Ser-356, i.e., the primary sites that had the highest degree of phosphorylation (Table 1), we found stronger NMR signal intensities. The proline-rich domain, on the other hand, behaved in a similar manner in nonphosphorylated and MARK2cat-phosphorylated Tau. Thus, the affinity of the proline-rich region for MTs is unaltered in Tau phosphorylated by MARK2cat. A sequence-specific alteration of MT binding of Tau by MARK2cat phosphorylation was further supported by experiments using a partially phosphorylated Tau protein (~72 ± 2% phosphorylated Ser-262), which allows the analysis of NMR line broadening of nonphosphorylated and phosphorylated Tau in a single sample. The line broadening detected in this sample for the nonphosphorylated form (Figure 5B) was very similar to that observed in the completely nonphosphorylated protein (Figure 5A,B).

In the next step we probed the phosphorylation-dependent modulation of Tau–microtubule interactions outside the repeat domain. For this purpose, we prepared a variant of 2N4R Tau, in which residues Ser-199, Ser-202, Thr-205, Thr-212, Ser-214, Ser-396, and Ser-404 were mutated to glutamic acid (called 2N4R Tau-7E hereafter). 2N4R Tau-7E mimics phosphorylation at the sites, which form epitopes for the Alzheimer's diagnostic antibodies AT8, AT100, and PHF1.[37] Comparison of MT-induced NMR line broadening in wild-type 2N4R Tau and Tau-7E showed that pseudophosphorylation at the AT8, AT100, and PHF1 sites slightly attenuated NMR line broadening in the proline-rich domains, while the repeat domain remained largely unaffected (Figure 5C). Notably, only small changes in NMR signal broadening were observed in R′ downstream of the repeats despite phosphorylation at Ser-396 and Ser-404. In summary, phosphorylation at the KXGS motifs more strongly attenuated the Tau–MT interaction than that of the Tau-7E mutant, and the effects of phosphorylation within and outside of the repeat domain on the Tau–MT interaction were largely independent.

■ DISCUSSION

Identification of Novel and Confirmation of Previously Detected Phosphorylation Sites. Phosphorylation of Ser-262 is an important post-translational modification of Tau that regulates MT dynamics[15] and the accessibility of Tau for other kinases.[18] Phosphorylation at Ser-262 is detected *in vivo*,[38] and Ser-262 together with Ser-356 is one of the few

phosphorylation sites identified within the repeat domain of AD brain-derived paired helical filaments.[39] Although several kinases can phosphorylate Ser-262 within Tau, only the MARKs are specific for this site and the other KXGS motifs.[11,24] MARKs predominantly target Ser-262 and Ser-356 within the KIGS motifs of Tau, while the two KCGS motifs in repeats R2 and R3 are less phosphorylated.[24,28] Despite numerous threonine residues in Tau (up to 35 residues), our quantitative NMR-based analysis detected no phosphorylation of this amino acid type, suggesting that MARK2 is highly specific for serine residues. The analysis confirmed Ser-262 (in R1) and Ser-356 (in R4) as primary phosphorylation sites of MARK2 but also identified Ser-324 (in R3) as a third primary site (Figure 1 and Table 1). All three sites are not subject to alternative splicing and are therefore contained in all Tau isoforms.

The NMR-based analysis revealed four additional serines that are phosphorylated by the catalytic domain of MARK2, albeit at lower efficiency because of their non-KXGS type (Figure 1 and Table 1). Whereas it is known that MARKs can phosphorylate Ser-305,[28] no study has reported the phosphorylation of Ser-352, Ser-413, and Ser-416 by MARK2. These three sites are known *in vitro* targets of casein kinase 1/2, cAMP-dependent protein kinase (PKA), glycogen synthase kinase-3, phosphorylase kinase, and calcium/calmodulin-dependent protein kinase II (CAMKII).[39−41] The physiological significance of phosphorylation of non-KXGS motifs by MARK2 is currently unclear. Under nonpathological conditions, these sites might not be phosphorylated in neurons[39] because of the low efficiency of MARK2 and the action of phosphatases. However, during disease when the activity of phosphatases is reduced,[42] phosphorylation levels at these sites may become relevant. In support of this hypothesis, Ser-413 and Ser-416 were detected in brain-derived PHF Tau.[39] Phosphorylation of Ser-416 by CAMKII and PKA was shown to be essential for Aβ-mediated cell cycle re-entry in neurons, a critical event in AD pathogenesis.[43] Additionally, phosphorylation of Ser-413 and Ser-416 might influence the truncation of Tau at Glu-391 and Asp-421 and in this way contribute to the pathogenesis of tauopathies.[44−46]

Kinetic Analysis of Tau Phosphorylation and Substrate Specificity. A unique advantage of the NMR-based analysis of phosphorylation is the ability to determine the kinetics of phosphorylation at all sites in a single sample without any purification. The approach therefore allows direct comparison of the efficiency of phosphorylation at distinct sites. In line with the observed saturation levels (Table 1), faster phosphorylation kinetics were found for the two KIGS motifs (residues 259−262 and 353−356) than for the serine residues in KCGS sequences (Figure 1D). Previous studies suggested that efficient recognition by MARK2 requires specific interactions between the catalytic cleft and the substrate.[47] One of these anchor points involves a salt bridge, in the case of the complex of MARK2 with the peptide inhibitor CagA W, from Arg-952 of CagA W to Glu-136 and Asp-139 of MARK2.[47] Arg-952 of CagA W corresponds to the lysine in the KXGS motif of Tau (Figure 1C). The more hydrophobic nature of isoleucine at position $i − 2$ (relative to the phosphorylation site) in the two KIGS motifs further favors binding to the hydrophobic pocket of MARK2. The fact that the two KIGS (as well as the two KCGS) motifs were phosphorylated at different rates indicates that residues flanking the motifs also influence the phosphorylation reaction. The

amino acid sequence also supports phosphorylation at the four non-KXGS sites: Ser-416 and Ser-305 are preceded by a glycine, i.e., the same residue present in the KXGS motif (Figure 1C).

The N-Terminal Tail of Tau Is the Major Binding Site for MARK2. Titration of Tau with MARK2cat provided further insights into the nature of MARK2−substrate interactions. Stretches in 2N4R Tau with a higher abundance of hydrophobic residues displayed more line broadening than regions that are deprived of hydrophobic residues, e.g., residues 45−240. The strongest interaction, however, was observed for residues 8−33 (Figure 2), indicating that MARK2 preferentially binds to the N-terminal tail of Tau upstream of the alternatively spliced inserts N1 and N2. Thus, the potential docking site of MARK2 is present on all Tau isoforms. No sites phosphorylated by MARK2 are found in this region, but it is remarkable that the N-terminal residues comprise the interaction site for various protein partners such as Fyn[48] and the p150 subunit of the dynactin complex.[49] Furthermore, it has been shown that residues 2−18, the so-called phosphatase-activating domain,[50] are critically involved in inhibition of fast axonal transport because of an interaction with protein phosphatase 1 and might therefore contribute to the toxicity of Tau filaments.[51]

The N-terminal tail (or "projection domain") of MT-bound Tau protrudes away from the MT surface. We hypothesize that similar to the binding of PKA to the N-terminus of MAP2,[52] the projection domain of Tau may serve as an anchor site for MARK2 localizing it to the vicinity of axonal MTs. Transient interactions of the N-terminus with the repeat domain of Tau[9,27] may further bring MARK2 into close contact with the KXGS motifs, thus favoring their phosphorylation (Figure 6).
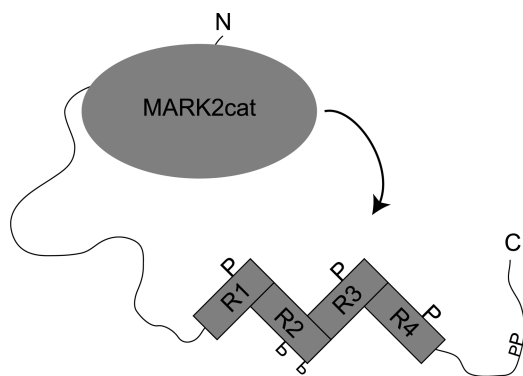

Figure 6. Hypothetical model for the binding of MARK2cat to Tau and its phosphorylation. MARK2cat preferentially binds to the N-terminal tail of Tau. Transient interactions of the N-terminal tail and the repeat domain favor phosphorylation of the KXGS motifs within the pseudorepeats by MARK2cat. MARK2cat phosphorylation sites are highlighted with a capital P (larger letters are used for primary sites Ser-262 in R1, Ser-324 in R3, and Ser-356 in R4).

Phosphorylation by MARK2 Induces Localized but No Global Structural Changes. Despite its intrinsically disordered nature, the ensemble of Tau structures contains globally compacted conformers.[9,10] We previously showed that pseudophosphorylation at the AT8, AT100, and PHF1 epitopes attenuates long-range interactions because of a weakened electrostatic attraction of the proline-rich region for the negatively charged N-terminal domain.[27] In contrast, MARK2 phosphorylation within the repeat domain did not change the

PRE-induced line broadening (Figure 3D) and thus did not modulate the global Tau structure.

Phosphorylation, however, did change the structure next to the phosphorylation sites (Figure 3A−C). A detailed analysis of NMR chemical shifts, residual dipolar couplings, and NOE contacts revealed that phosphorylation at Ser-262 pushes residues 264−267 toward helical and turnlike conformations (Figure 4). The increase in helical propensity is consistent with previous results that demonstrated a stabilization of α-helices through phosphorylation at their N-termini. This was rationalized through favorable electrostatic interaction of the phosphate group with the helix dipole, and through possible hydrogen bonds of the phosphate group to main chain amide groups.[53] Additionally, Ser-262 phosphorylation rigidifies the protein backbone at the phosphorylation site (Figure 4I), demonstrating that phosphorylation by MARK2 modulates both the structure and dynamics of Tau. These modulations may be the reason for the enhanced intrinsic acetyltransferase activity of Tau after phosphorylation of the KXGS motifs, which results in autoacteylation of Tau, thus promoting Tau toxicity.[54,55]

Tau's MT-Binding Hot Spots Are Regulated Independently by Phosphorylation. A major physiological function of Tau is to regulate MT dynamics.[3] This process is influenced by Tau phosphorylation, particularly at Ser-262.[15,56] We previously showed that four regions in 2N4R Tau are strongly involved in MT binding: residues 225−231, 245−253, 275−287, and 306−318.[9] In addition, residues 170−181 and 370−381 contribute to the MT interaction. The interaction studies with different phosphorylated Tau species now revealed that Tau's MT-binding sites act largely independently of each other. Pseudophosphorylation at AT8, AT100, and PHF1 epitopes reduced the affinity of the proline-rich domain P2, which harbors the AT8 and AT100 phosphorylation sites, but hardly affected the interaction of the repeat domain with MTs (Figure 5C). In contrast, phosphorylation at the KXGS motifs by MARK2cat attenuated binding of the repeat domain to MTs but had an only limited influence on the proline-rich region (Figure 5A,B). Thus, the proline-rich region is unaffected by phosphorylation through MARK2 and can still bind to MTs, despite an overall decrease in affinity.[57] An interaction with MTs solely mediated through the repeat-flanking P2 domain, however, is nonproductive and does not result in MT assembly or MT stabilization.[58]

The NMR data are therefore in agreement with previous reports demonstrating that Ser-262-phosphorylated Tau is still able to bind MTs.[15,38] Phosphorylation of Ser-262 is insufficient to abolish the Tau−MT interaction. Phosphorylation at additional sites is required for inhibition of MT binding.[56] It thus seems possible that Ser-324 and Ser-356 have important accessory roles. Both Ser-324 and Ser-356 were efficiently phosphorylated by MARK2 (Table 1), and their phosphorylation weakened the MT-induced line broadening of nearby residues (Figure 5A,B). In particular, Ser-356 phosphorylation may regulate the MT interaction of residues 370−381 in R′, a region that together with the repeat domain possesses significant binding strength for MTs.[57]

Potential Mechanism for the Phosphorylation-Induced Decrease in Tau's Affinity for MTs. A possible molecular mechanism for a phosphorylation-induced decrease in the level of binding of Tau to MTs could be a phosphorylation-induced conformational change in Tau. For instance, conformational alterations to less globally compacted

conformations were observed upon pseudophosphorylation of the proline-rich region.[27] Surprisingly, despite the reduced affinity for MTs, phosphorylation of Tau by MARK2 induced only limited structural changes (Figures 3 and 4). The local nature of the structural changes then poses the question of how phosphorylation in the repeat domain decreases the affinity of Tau for MTs. A potential hypothesis is therefore that the observed changes, which are located in regions connecting different MT-binding hot spots, might interfere with a conformational rearrangement that is required for MT binding. In addition, phosphorylation in the repeat domain reduces the flexibility of the Tau backbone, further disfavoring conformational changes. Finally, electrostatic repulsion between the phosphate group and the negatively charged MT surface will contribute to a decrease in the affinity of Tau for MTs.

In summary, we showed that MARK2 binds to the N-terminal region of Tau and can phosphorylate eight sites with distinct kinetics, where the three primary target sites are the KXGS motifs of R1, R3, and R4. Phosphorylation results in local structural changes upstream of the phosphorylation sites, in regions connecting MT interaction sequences that are regulated independently by phosphorylation. The finding that phosphorylation of Tau by MARK2 influences the molecular properties of Tau suggests that regulation of MARK2 might be an entry point for combating Alzheimer's disease.

■ ASSOCIATED CONTENT

Ⓢ Supporting Information

Further experimental procedures detailing the synthesis of proteins and peptides, NMR experiments used for assignment, PRE data and RDC acquisition, and a description of the *flexible-meccano*/ASTEROIDS approach. This material is available free of charge via the Internet at http://pubs.acs.org.

■ AUTHOR INFORMATION

Corresponding Author

*German Center for Neurodegenerative Diseases (DZNE) and Max Planck Institute for Biophysical Chemistry, Am Fassberg 11, 37077 Göttingen, Germany. Telephone: +49-551-201-2220. E-mail: markus.zweckstetter@dzne.de.

Notes

The authors declare no competing financial interest.

■ ACKNOWLEDGMENTS

■ ABBREVIATIONS

AD, Alzheimer's disease; HSQC, heteronuclear single-quantum coherence; MAP, microtubule-associated protein; MARK2, microtubule-associated protein/microtubule affinity-regulating kinase 2; MARK2cat, catalytic domain of MARK2; MICS, motif identification from chemical shifts; MT, microtubule; MTSL, *S*-(2,2,5,5-tetramethyl-2,5-dihydro-1*H*-pyrrol-3-yl)methyl methane-sulfonothioate; NMR, nuclear magnetic resonance; PHF, paired helical filament; PRE, paramagnetic relaxation enhancement; NOE, nuclear Overhauser effect; RDC, residual dipolar coupling; 2N4R Tau, 441-residue Tau.

■ REFERENCES

(1) Avila, J., Lucas, J. J., Perez, M., and Hernandez, F. (2004) Role of Tau Protein in Both Physiological and Pathological Conditions. *Physiol. Rev. 84*, 361−384.

(2) Buee, L., Bussiere, T., Buee-Scherrer, V., Delacourte, A., and Hof, P. R. (2000) Tau protein isoforms, phosphorylation and role in neurodegenerative disorders. *Brain Res. Rev. 33*, 95−130.

(3) Weingarten, M. D., Lockwood, A. H., Hwo, S. Y., and Kirschner, M. W. (1975) A protein factor essential for microtubule assembly. *Proc. Natl. Acad. Sci. U.S.A. 72*, 1858−1862.

(4) Caceres, A., Potrebic, S., and Kosik, K. S. (1991) The effect of tau antisense oligonucleotides on neurite formation of cultured cerebellar macroneurons. *J. Neurosci. 11*, 1515−1523.

(5) Lee, G., and Leugers, C. J. (2012) Tau and Tauopathies. *Prog. Mol. Biol. Transl. Sci. 107*, 263−293.

(6) Schweers, O., Schönbrunn-Hanebeck, E., Marx, A., and Mandelkow, E. (1994) Structural studies of tau protein and Alzheimer paired helical filaments show no evidence for β-structure. *J. Biol. Chem. 269*, 24290−24297.

(7) Lindwall, G., and Cole, R. D. (1984) The purification of tau protein and the occurrence of two phosphorylation states of tau in brain. *J. Biol. Chem. 259*, 12241−12245.

(8) Uversky, V. N., and Dunker, A. K. (2010) Understanding protein non-folding. *Biochim. Biophys. Acta 1804*, 1231−1264.

(9) Mukrasch, M. D., Bibow, S., Korukottu, J., Jeganathan, S., Biernat, J., Griesinger, C., Mandelkow, E., and Zweckstetter, M. (2009) Structural Polymorphism of 441-Residue Tau at Single Residue Resolution. *PLoS Biol. 7*, e1000034.

(10) Jeganathan, S., von Bergen, M., Brutlach, H., Steinhoff, H.-J., and Mandelkow, E. (2006) Global Hairpin Folding of Tau in Solution. *Biochemistry 45*, 2283−2293.

(11) Martin, L., Latypova, X., Wilson, C. M., Magnaudeix, A., Perrin, M.-L., Yardin, C., and Terro, F. (2012) Tau protein kinases: Involvement in Alzheimer's disease. *Ageing Res. Rev. 12*, 289−309.

(12) Illenberger, S., Zheng-Fischhöfer, Q., Preuss, U., Stamer, K., Baumann, K., Trinczek, B., Biernat, J., Godemann, R., Mandelkow, E.-M., and Mandelkow, E. (1998) The Endogenous and Cell Cycle-dependent Phosphorylation of tau Protein in Living Cells: Implications for Alzheimer's Disease. *Mol. Biol. Cell 9*, 1495−1512.

(13) Cho, J.-H., and Johnson, G. V. W. (2004) Primed phosphorylation of tau at Thr231 by glycogen synthase kinase 3β (GSK3β) plays a critical role in regulating tau's ability to bind and stabilize microtubules. *J. Neurochem. 88*, 349−358.

(14) Lu, P.-J., Wulf, G., Zhou, X. Z., Davies, P., and Lu, K. P. (1999) The prolyl isomerase Pin1 restores the function of Alzheimer-associated phosphorylated tau protein. *Nature 399*, 784−788.

(15) Biernat, J., Gustke, N., Drewes, G., Mandelkow, E., and Mandelkow, E. (1993) Phosphorylation of Ser262 strongly reduces binding of tau to microtubules: Distinction between PHF-like immunoreactivity and microtubule binding. *Neuron 11*, 153−163.

(16) Utton, M. A., Vandecandelaere, A., Wagner, U., Reynolds, C. H., Gibb, G. M., Miller, C. C., Bayley, P. M., and Anderton, B. H. (1997) Phosphorylation of tau by glycogen synthase kinase 3β affects the ability of tau to promote microtubule self-assembly. *Biochem. J. 323*, 741−747.

(17) Amniai, L., Barbier, P., Sillen, A., Wieruszeski, J.-M., Peyrot, V., Lippens, G., and Landrieu, I. (2009) Alzheimer disease specific phosphoepitopes of Tau interfere with assembly of tubulin but not binding to microtubules. *FASEB J. 23*, 1146−1152.

(18) Bertrand, J., Plouffe, V., Sénéchal, P., and Leclerc, N. (2010) The pattern of human tau phosphorylation is the result of priming and feedback events in primary hippocampal neurons. *Neuroscience 168*, 323−334.

(19) Gustke, N., Steiner, B., Mandelkow, E. M., Biernat, J., Meyer, H. E., Goedert, M., and Mandelkow, E. (1992) The Alzheimer-like phosphorylation of tau protein reduces microtubule binding and involves Ser-Pro and Thr-Pro motifs. *FEBS Lett. 307*, 199−205.

(20) Biernat, J., and Mandelkow, E.-M. (1999) The Development of Cell Processes Induced by tau Protein Requires Phosphorylation of

Serine 262 and 356 in the Repeat Domain and Is Inhibited by Phosphorylation in the Proline-rich Domains. *Mol. Biol. Cell* 10, 727−740.

(21) Chatterjee, S., Sang, T.-K., Lawless, G. M., and Jackson, G. R. (2009) Dissociation of tau toxicity and phosphorylation: Role of GSK-3β, MARK and Cdk5 in a *Drosophila* model. *Hum. Mol. Genet.* 18, 164−177.

(22) Yu, W., Polepalli, J., Wagh, D., Rajadas, J., Malenka, R., and Lu, B. (2012) A critical role for the PAR-1/MARK-tau axis in mediating the toxic effects of Aβ on synapses and dendritic spines. *Hum. Mol. Genet.* 21, 1384−1390.

(23) Hanger, D. P., Anderton, B. H., and Noble, W. (2009) Tau phosphorylation: The therapeutic challenge for neurodegenerative disease. *Trends Mol. Med.* 15, 112−119.

(24) Yoshida, H., and Goedert, M. (2012) Phosphorylation of microtubule-associated protein tau by AMPK-related kinases. *J. Neurochem.* 120, 165−176.

(25) Matenia, D., and Mandelkow, E.-M. (2009) The tau of MARK: A polarized view of the cytoskeleton. *Trends Biochem. Sci.* 34, 332−342.

(26) Landrieu, I., Lacosse, L., Leroy, A., Wieruszeski, J.-M., Trivelli, X., Sillen, A., Sibille, N., Schwalbe, H., Saxena, K., Langer, T., and Lippens, G. (2006) NMR Analysis of a Tau Phosphorylation Pattern. *J. Am. Chem. Soc.* 128, 3575−3583.

(27) Bibow, S., Ozenne, V., Biernat, J., Blackledge, M., Mandelkow, E., and Zweckstetter, M. (2011) Structural Impact of Proline-Directed Pseudophosphorylation at AT8, AT100, and PHF1 Epitopes on 441-Residue Tau. *J. Am. Chem. Soc.* 133, 15842−15845.

(28) Drewes, G., Trinczek, B., Illenberger, S., Biernat, J., Schmitt-Ulms, G., Meyer, H. E., Mandelkow, E.-M., and Mandelkow, E. (1995) Microtubule-associated Protein/Microtubule Affinity-regulating Kinase (p110mark): A novel protein kinase that regulates tau-microtubule interactions and dynamic instability by phosphorylation at the Alzheimer-specific site serine 262. *J. Biol. Chem.* 270, 7679−7688.

(29) Timm, T., Li, X.-Y., Biernat, J., Jiao, J., Mandelkow, E., Vandekerckhove, J., and Mandelkow, E.-M. (2003) MARKK, a Ste20-like kinase, activates the polarity-inducing kinase MARK/PAR-1. *EMBO J.* 22, 5090−5101.

(30) Schneider, A., Biernat, J., von Bergen, M., Mandelkow, E., and Mandelkow, E. M. (1999) Phosphorylation that Detaches Tau Protein from Microtubules (Ser262, Ser214) Also Protects It against Aggregation into Alzheimer Paired Helical Filaments. *Biochemistry* 38, 3549−3558.

(31) O'Connell, M. R., Gamsjaeger, R., and Mackay, J. P. (2009) The structural analysis of protein−protein interactions by NMR spectroscopy. *Proteomics* 9, 5224−5232.

(32) Huang, J. R., Gentner, M., Vajpai, N., Grzesiek, S., and Blackledge, M. (2012) Residual dipolar couplings measured in unfolded proteins are sensitive to amino-acid-specific geometries as well as local conformational sampling. *Biochem. Soc. Trans.* 40, 989−994.

(33) Fischer, D., Mukrasch, M. D., Biernat, J., Bibow, S., Blackledge, M., Griesinger, C., Mandelkow, E., and Zweckstetter, M. (2009) Conformational Changes Specific for Pseudophosphorylation at Serine 262 Selectively Impair Binding of Tau to Microtubules. *Biochemistry* 48, 10047−10055.

(34) Shen, Y., and Bax, A. (2012) Identification of helix capping and β-turn motifs from NMR chemical shifts. *J. Biomol. NMR* 52, 211−232.

(35) Ozenne, V., Schneider, R., Yao, M., Huang, J.-r., Salmon, L., Zweckstetter, M., Jensen, M. R., and Blackledge, M. (2012) Mapping the Potential Energy Landscape of Intrinsically Disordered Proteins at Amino Acid Resolution. *J. Am. Chem. Soc.* 134, 15138−15148.

(36) Mukrasch, M. D., von Bergen, M., Biernat, J., Fischer, D., Griesinger, C., Mandelkow, E., and Zweckstetter, M. (2007) The "Jaws" of the Tau-Microtubule Interaction. *J. Biol. Chem.* 282, 12230−12239.

(37) Jeganathan, S., Hascher, A., Chinnathambi, S., Biernat, J., Mandelkow, E.-M., and Mandelkow, E. (2008) Proline-directed Pseudo-phosphorylation at AT8 and PHF1 Epitopes Induces a Compaction of the Paperclip Folding of Tau and Generates a Pathological (MC-1) Conformation. *J. Biol. Chem.* 283, 32066−32076.

(38) Seubert, P., Mawal-Dewan, M., Barbour, R., Jakes, R., Goedert, M., Johnson, G. V. W., Litersky, J. M., Schenk, D., Lieberburg, I., Trojanowski, J. Q., and Lee, V. M. Y. (1995) Detection of Phosphorylated Ser in Fetal Tau, Adult Tau, and Paired Helical Filament Tau. *J. Biol. Chem.* 270, 18917−18922.

(39) Hanger, D. P., Byers, H. L., Wray, S., Leung, K.-Y., Saxton, M. J., Seereeram, A., Reynolds, C. H., Ward, M. A., and Anderton, B. H. (2007) Novel Phosphorylation Sites in Tau from Alzheimer Brain Support a Role for Casein Kinase 1 in Disease Pathogenesis. *J. Biol. Chem.* 282, 23645−23654.

(40) Paudel, H. K. (1997) The Regulatory Ser262 of Microtubule-associated Protein Tau Is Phosphorylated by Phosphorylase Kinase. *J. Biol. Chem.* 272, 1777−1785.

(41) Steiner, B., Mandelkow, E. M., Biernat, J., Gustke, N., Meyer, H. E., Schmidt, B., Mieskes, G., Söling, H. D., Drechsel, D., and Kirschner, M. W. (1990) Phosphorylation of microtubule-associated protein tau: identification of the site for Ca²⁺-calmodulin dependent kinase and relationship with tau phosphorylation in Alzheimer tangles. *EMBO J.* 9, 3593−3544.

(42) Liu, F., Grundke-Iqbal, I., Iqbal, K., and Gong, C.-X. (2005) Contributions of protein phosphatases PP1, PP2A, PP2B and PP5 to the regulation of tau phosphorylation. *Eur. J. Neurosci.* 22, 1942−1950.

(43) Seward, M. E., Swanson, E., Norambuena, A., Reimann, A., Cochran, J. N., Li, R., Roberson, E. D., and Bloom, G. S. (2013) Amyloid-β signals through tau to drive ectopic neuronal cell cycle re-entry in Alzheimer's disease. *J. Cell Sci.* 126, 1278−1286.

(44) Zilka, N., Filipcik, P., Koson, P., Fialova, L., Skrabana, R., Zilkova, M., Rolkova, G., Kontsekova, E., and Novak, M. (2006) Truncated tau from sporadic Alzheimer's disease suffices to drive neurofibrillary degeneration in vivo. *FEBS Lett.* 580, 3582−3588.

(45) Rissman, R. A., Poon, W. W., Blurton-Jones, M., Oddo, S., Torp, R., Vitek, M. P., LaFerla, F. M., Rohn, T. T., and Cotman, C. W. (2004) Caspase-cleavage of tau is an early event in Alzheimer disease tangle pathology. *J. Clin. Invest.* 114, 121−130.

(46) Guillozet-Bongaarts, A. L., Glajch, K. E., Libson, E. G., Cahill, M. E., Bigio, E., Berry, R. W., and Binder, L. I. (2007) Phosphorylation and cleavage of tau in non-AD tauopathies. *Acta Neuropathol.* 113, 513−520.

(47) Nesic, D., Miller, M. C., Quinkert, Z. T., Stein, M., Chait, B. T., and Stebbins, C. E. (2010) *Helicobacter pylori* CagA inhibits PAR1-MARK family kinases by mimicking host substrates. *Nat. Struct. Mol. Biol.* 17, 130−132.

(48) Usardi, A., Pooler, A. M., Seereeram, A., Reynolds, C. H., Derkinderen, P., Anderton, B., Hanger, D. P., Noble, W., and Williamson, R. (2011) Tyrosine phosphorylation of tau regulates its interactions with Fyn SH2 domains, but not SH3 domains, altering the cellular localization of tau. *FEBS J.* 278, 2927−2937.

(49) Magnani, E., Fan, J., Gasparini, L., Golding, M., Williams, M., Schiavo, G., Goedert, M., Amos, L. A., and Spillantini, M. G. (2007) Interaction of tau protein with the dynactin complex. *EMBO J.* 26, 4546−4554.

(50) Kanaan, N. M., Morfini, G. A., LaPointe, N. E., Pigino, G. F., Patterson, K. R., Song, Y., Andreadis, A., Fu, Y., Brady, S. T., and Binder, L. I. (2011) Pathogenic Forms of Tau Inhibit Kinesin-Dependent Axonal Transport through a Mechanism Involving Activation of Axonal Phosphotransferases. *J. Neurosci.* 31, 9858−9868.

(51) LaPointe, N. E., Morfini, G., Pigino, G., Gaisina, I. N., Kozikowski, A. P., Binder, L. I., and Brady, S. T. (2009) The amino terminus of tau inhibits kinesin-dependent axonal transport: Implications for filament toxicity. *J. Neurosci. Res.* 87, 440−451.

(52) Vallee, R. B., DiBartolomeis, M. J., and Theurkauf, W. E. (1981) A protein kinase bound to the projection portion of MAP 2 (microtubule-associated protein 2). *J. Cell Biol.* 90, 568−576.

(53) Andrew, C. D., Warwicker, J., Jones, G. R., and Doig, A. J. (2002) Effect of Phosphorylation on α-Helix Stability as a Function of Position. *Biochemistry* 41, 1897−1905.

(54) Cohen, T. J., Friedmann, D., Hwang, A. W., Marmorstein, R., and Lee, V. M. Y. (2013) The microtubule-associated tau protein has intrinsic acetyltransferase activity. *Nat. Struct. Mol. Biol. 20*, 756−762.

(55) Irwin, D. J., Cohen, T. J., Grossman, M., Arnold, S. E., Xie, S. X., Lee, V. M. Y., and Trojanowski, J. Q. (2012) Acetylated tau, a novel pathological signature in Alzheimer's disease and other tauopathies. *Brain 135*, 807−818.

(56) Sengupta, A., Kabat, J., Novak, M., Wu, Q., Grundke-Iqbal, I., and Iqbal, K. (1998) Phosphorylation of Tau at Both Thr 231 and Ser 262 Is Required for Maximal Inhibition of Its Binding to Microtubules. *Arch. Biochem. Biophys. 357*, 299−309.

(57) Gustke, N., Trinczek, B., Biernat, J., Mandelkow, E. M., and Mandelkow, E. (1994) Domains of Tau Protein and Interactions with Microtubules. *Biochemistry 33*, 9511−9522.

(58) Preuss, U., Biernat, J., Mandelkow, E. M., and Mandelkow, E. (1997) The 'jaws' model of tau-microtubule interaction examined in CHO cells. *J. Cell Sci. 110*, 789−800.